

Growth, synthesis, structural and optical properties of pure ZnO by colloidal solution route

Vipul Shukla, Dr.Amit Patel,
Gujarat Technological University, Chandkheda, Ahmedabad –382424 Gujarat,
Government Engineering college, Godhra –389001 Gujarat

Abstract: Zinc oxide thin films were deposited on glass substrate from aqueous solution of ZnCl_2 and NH_3 by chemical bath deposition method. ZnO nanoparticles were generated by zinc chloride as single source precursor. Thermal behavior of the precursor showed a considerable weight loss at about 538°C by an exothermic reaction with a maximum weight loss rate of 6% per min., complete decomposition of precursor was observed within 87 min with a heating rate of $25^\circ\text{C}/\text{min}$. TGA analysis of ZnO sample revealed three endothermic peaks around 160°C , 290°C and 538°C . These endothermic peaks are attributed to the loss of volatile surfactant, conversion of zinc hydroxide to zinc oxide nanoparticles and transformation of zinc oxide into zinc nanoparticles. The optical properties were studied using UV-Vis-NIR spectrometer for absorbance of the thin films. The morphology, crystallinity and structural properties are studied by X-ray diffraction (XRD). Also the morphology of the films studied by scanning electron microscope (SEM). XRD and SEM data suggest that good quality ZnO films are obtained. Structural analysis with XRD and SEM revealed that the formed films exhibit a wurtzite hexagonal phase. Refractive index is 1.02 – 1.07. Value of the real part of dielectric constant is 1.03- 1.16. The experimental pattern of the films show very fine peaks indicate a good crystallization. The band gap was 4.26, 4.28, 4.28, 4.29 and 4.30 eV for different number of coat.

Keywords: Zinc Oxide, Chemical bath deposition, Thin films, TGA, XRD, Scanning Electron Microscopy(SEM), UV-Vis-NIR.

I INTRODUCTION

ZnO thin film is one of the II-VI compound semiconductors and is composed of hexagonal wurtzite crystal structure. ZnO thin film presents investigating optical, acoustical and electrical properties which meet extent applications in the fields of electronics, optoelectronics and sensors. ZnO thin film is applied to the transparent conductive film and the solar cell window because of the high optical transmittance in the visible region. In the last year's low size (Nano,micro)materials have interesting attention due to their size dependent properties and wide range of applications in different fields such as industry, health and environment[1-5]. ZnO is one of the II-VI semiconductors, it has a direct wide band gap(3.37 eV) and excitation energy (60 meV) [6,7], has great attention for researchers because of its electrical and optical properties which make it important material in many applications such as solar cell, chemical sensors, electroluminescent devices and ultraviolet laser diodes[8-9]. Also ZnO have been studied as the active channel in manufacturing and development transistors according to its n-type electric properties, very good thermal stability and can be well oriented crystalline on different substrates [10]. Since the control of the size and shape of nanostructure materials plays main role and great effect on the physical properties of the materials[10,11], several methods and techniques [11] are used to synthesize different materials including ZnO Nanostructures, such as Pulse Laser Deposition (PLD), Chemical Vapor Deposition (CVD), Chemical Bath Deposition (CBD), Hydrothermal and chemical reactions.[12]

The chemical bath deposition technique is simple cost; effective, reproducible and the material are readily available. As compared to other oxide material ZnO material is much cheap and easily available material. The presence work depend the chemical method due to its simplicity in requirements. Another advantage of the CBD method over other method is that the film can be deposited at different shapes and size of substrates.

II EXPERIMENTAL PROCEDURE

The ZnO thin films were prepared by chemical bath technique. The reaction bath is composed of ZnCl_2 used as precursor. For deposition of the film, commercial quality glass microscope slides of dimension $16\text{ mm} \times 26\text{ mm} \times 1\text{ mm}$ are used. Prior to use, these glass slides were soaked in aquaregia, a mixture of concentrated HCl. They were removed after 24 h and washed thoroughly in cold detergent solution, rinsed in distilled water and drip dried in air. The properly degreased and cleaned substrate surface has the advantage of producing highly adhesive and uniform film.

The reagents used in this experiment were zinc chloride, aqueous ammonia. 0.1 M of zinc chloride was prepared and small drops of ammonia were added and stirred continuously using a magnetic stirrer to obtain optimum pH of 9.6 for this deposition. 80 ml solution of zinc chloride and aqueous ammonia were put in 100 ml beaker and the substrates whose surface had been prepared under standard conditions were vertically suspended in the beaker and the solution was constantly stirred using magnetic stirrer in a water bath of constant temperature of 82°C . The substrate was immersed vertically at the centre of reaction bath in such a way it should not touch the walls of the beaker. The deposition time was 135 minutes. After 120 minutes the substrate with deposited thin films were removed, rinsed with distilled water and left to dry. The as-deposited ZnO thin films were also annealed at 250°C

in a furnace. By using the above given experimental method, thin films with variation in number of coats are grown on glass substrates.

We have characterized by employing thermo gravimetric analysis (TGA), scanning electron microscopy (SEM), XRD and UV-Vis-NIR. Thermo gravimetric analyzer (TGA, METTLER TOLEDO, Model: DSC3) was used to study the thermal stability of ZnO. SEM was used for morphological characterization of sample. The surface morphology of the white precipitate was determined by scanning electron microscope (SEM) JSM-6010LA. The structural parameters of the powder were determined using X-ray diffraction technique. The XRD patterns were recorded with D2 phaser Bruker advanced X-ray diffractometer using a Cu - K α radiation source ($\lambda = 1.547 \text{ \AA}$). Diffraction peaks were compared with those of the standard compounds reported in the JCPDS files (36-1451 card). The UV-Vis-NIR absorption spectra of the samples were recorded in the wave length range of 200 nm to 1200 nm using a Shimadzu UV-3600 UV-Vis-NIR spectrometer.

III RESULTS AND DISCUSSIONS

A. X-ray diffraction analysis of ZnO nanoparticles

The morphology, crystallinity and structural properties are studied by X-ray diffraction. The crystallographic structure of the films prepared at different coatings has been studied by XRD. XRD patterns exhibit strong peaks (100), (002), (101), (102), (110), (103) and (200) planes assigned to hexagonal wurtzite structure as shown in Fig.1. The experimental pattern of the films show very fine peaks indicate a good crystallization. The crystallite size of the ZnO nanoparticles was calculated by the X-ray line broadening method using the Scherrer's equation:

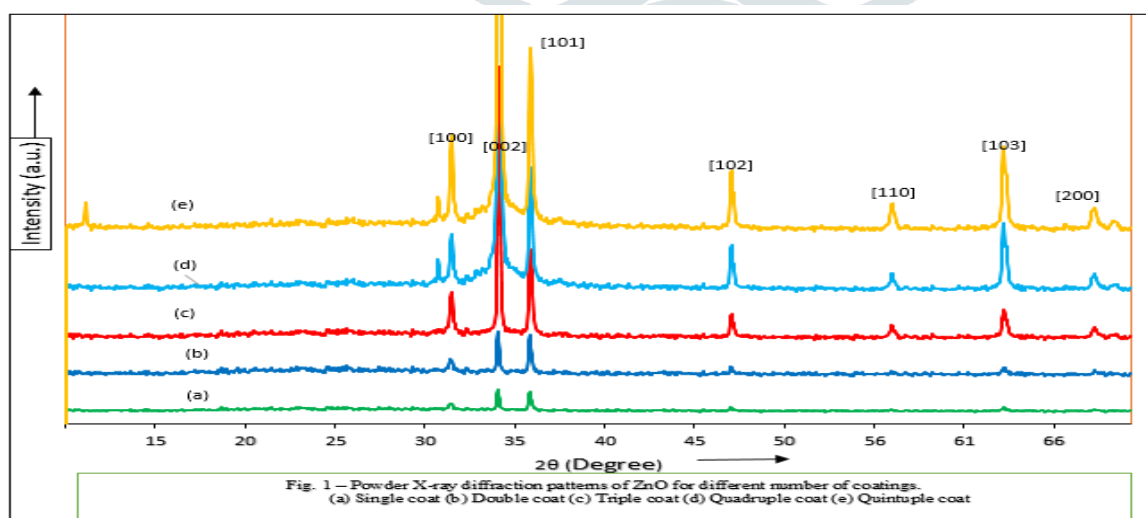
$$D = K\lambda / \beta \cos\theta$$

Where, D is the crystallite size, λ is the Cu -K α radiation of wavelength (1.547 \AA), K the shape factor (0.94), β is the full width at half maximum (FWHM) in radian and θ is the scattering angle. From the calculations, the average crystallite size of the ZnO nanoparticles was in the range from 38 nm to 44 nm and lattice strain gradually decrease as shown in Table 1.

Table 1 Average crystallite size of ZnO obtained from XRD using equation 1

| No. of Coat | Crystallite size D (nm) | Lattice Strain | Thickness of the film (μm) |
|----------------|---------------------------|----------------|---|
| Single coat | 38 | 0.0030 | 1.14 |
| Double Coat | 39 | 0.0029 | 3.91 |
| Triple Coat | 40 | 0.0028 | 6.07 |
| Quadruple coat | 42 | 0.0027 | 11.38 |
| Quintuple coat | 44 | 0.0026 | 14.78 |

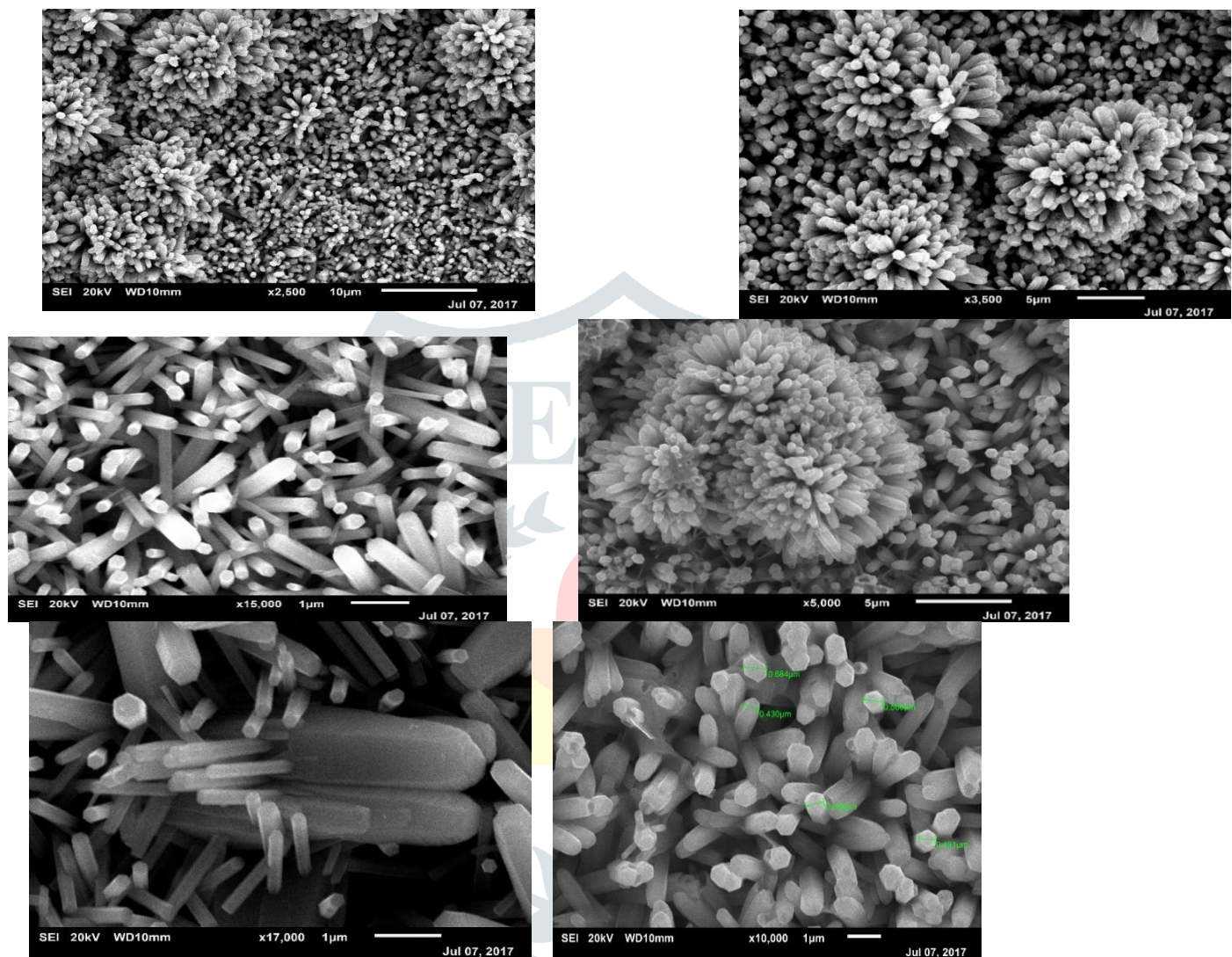
It can be seen from the XRD data that all samples are of single phase ZnO wurtzite structure (JCPDS, 36-1451) and the crystallinity of the films becomes better with increasing number of coat.



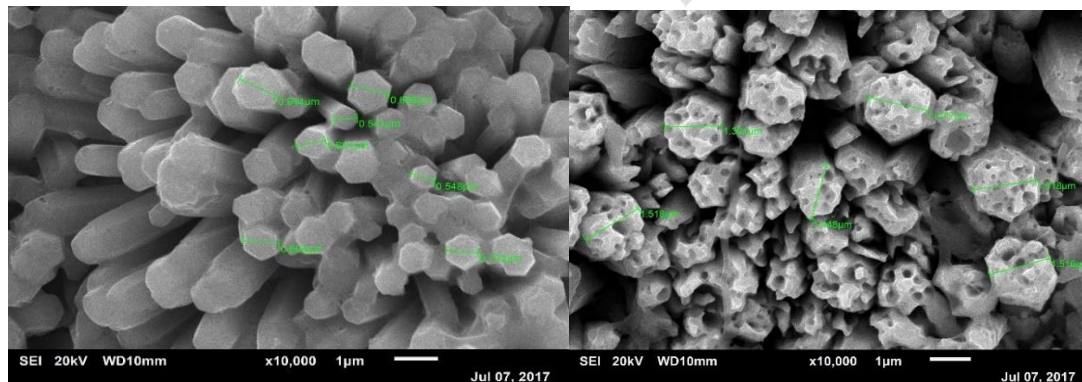
B. Morphological analysis

The growth parameters and ions concentration play a critical role for tuning the morphology of ZnO nanostructures grown during CBD process. The effect of coating on the evolution of ZnO film is further illustrated by SEM, as shown in Fig. 2.

The results of SEM observation shows that the diameter and length increase with number of coating increasing as shown in Fig. 3. It can clearly seen that the density of ZnO nanorods increases with the increasing of coat. Thickness of the thin films is also increases, which is measured from SEM analysis as shown in Table-1.



(Fig.2. SEM micrographs of ZnO films deposited on glass using chemical bath deposition)



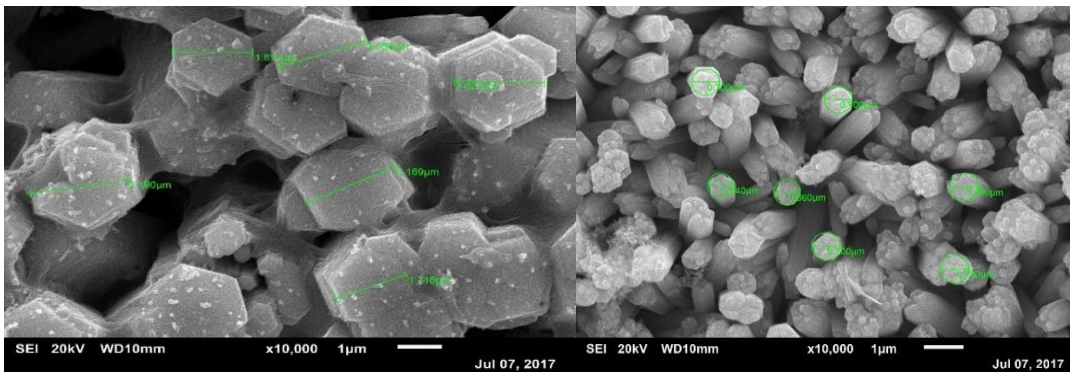


(Fig.3. SEM micrographs ZnO films deposited on glass using chemical bath deposition)

C. Optical study

The transmittance (T) can be calculated from the relationship (Pankove, 1971):

$$A = \log \left(\frac{1}{T} \right)$$

Where A is the absorbance and T is given (Pankove, 1971) by:

$$T = \frac{1}{10^A}$$

The reflectance (R) is calculated from the relation (Pankove, 1971):

$$A + R + T = 1 \quad \text{Or}$$

$$R = 1 - (A + T)$$

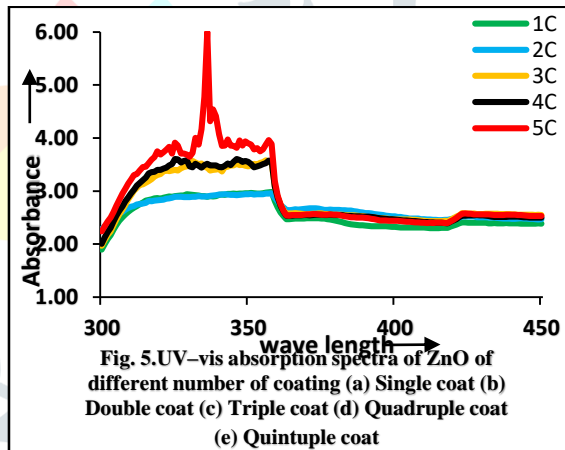
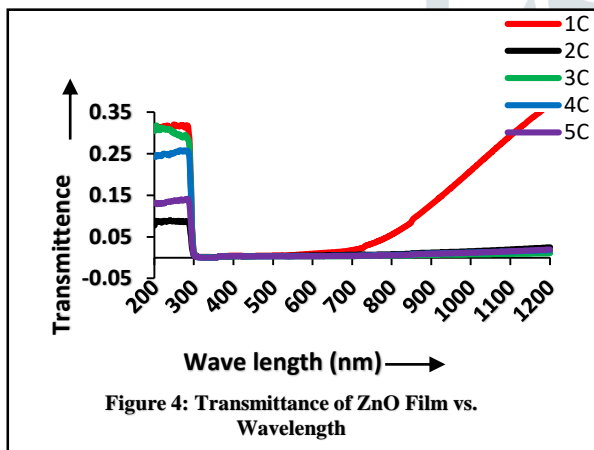


Fig. 5. UV-vis absorption spectra of ZnO of different number of coating (a) Single coat (b) Double coat (c) Triple coat (d) Quadruple coat (e) Quintuple coat

Figure 4 shows the optical transmission spectra of the ZnO films. The transmittance is high at 300 nm with drastic fall near the fundamental absorption.

Absorbance of the film: Optical experiments provide a good way of examining the properties of semiconductors. Particularly measuring the absorption coefficient for various energies gives information about the band gaps of the material. The optical information is obtained using spectrophotometer. The absorbance is obtained from the relation;

$$\alpha = \left[\left(\frac{2.30 A}{t} \right) \right]$$

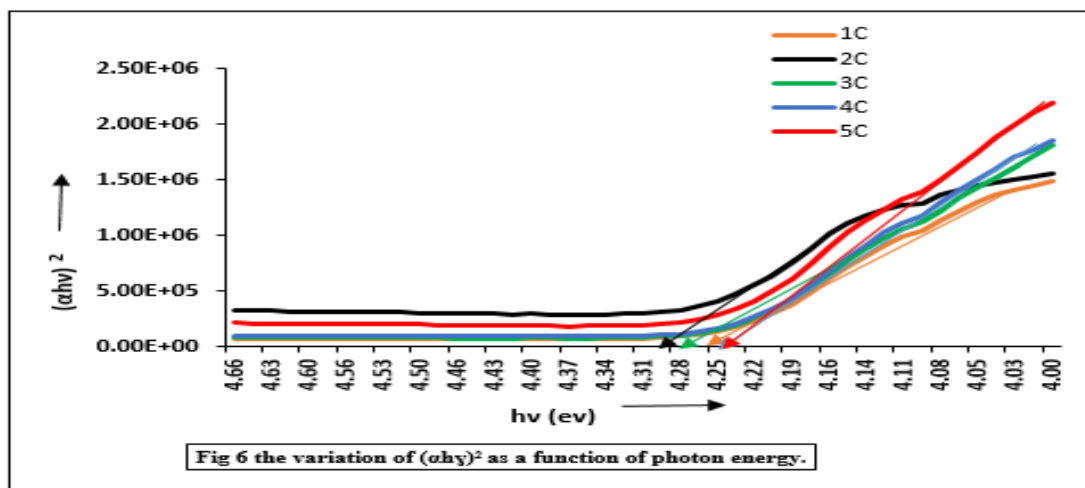
where t is the thickness of the deposited film, A is the absorbance.

The UV-visible absorption spectra of the samples are shown in Figure 5. All the samples have a strong absorption maximum below 370 nm. The absorption maximum for the quintuple coated thin film and it shifted to higher wavelengths. This red shift can be attributed to the agglomerations in the samples [14]. For the single coated thin film have low reflectance.

Bandgap Estimation: The bandgap of materials is a very important parameter that determines the application of the films. It is evaluated using the formula (Ezekoye & Okeke, 2005).

$$\alpha = \left(\frac{A}{hv} \right) (hv - E_g)^n$$

The band gap of the metallic oxide was determined by plotting (ahv)² as a function of hv, and extrapolating the linear portion of the curve to (ahv)² = 0 as shown in fig. 6. The value obtained for the optical band gap for single coat, double coat, triple coat, quadruple coat and quintuple coat is 4.26 eV, 4.28 eV, 4.28 eV, 4.29 eV and 4.30 eV respectively.



D. Thermogravimetric analysis

The thermal properties of precursor were determined by thermogravimetric analysis (TGA) and differential thermal analysis (DTA). Thermo Gravimetric Analysis was performed for the ZnO to study the thermal stability of materials. Sample was heated in an aluminum pan from room temperature to 600°C at a heating rate of 10°C/min. The TGA analyses (Fig. 6) revealed that the complex loses 7% of its weight at about 290°C attributed to desorption or removal of moisture and solvents, and 57% weight loss of its total weight at 538°C with a maximum weight loss rate of 6 % per min. indicating a fast rate of degradation of solid into volatile combustible products, proving the high thermal stability nature of ZnO. The TGA curve has a large exothermic peak at that temperature which may be attributed to the fact that volatile organic moieties generated by the dissociation of precursor react with O₂ to form CO₂ and H₂O. This is confirmed by the weight loss observed in the temperature region 0 to 800°C in the TGA curve, thus can be used for higher temperature applications also.

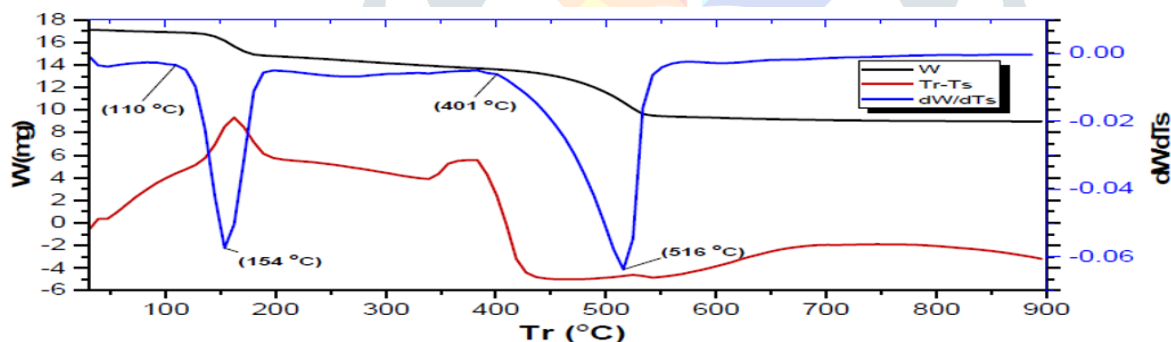


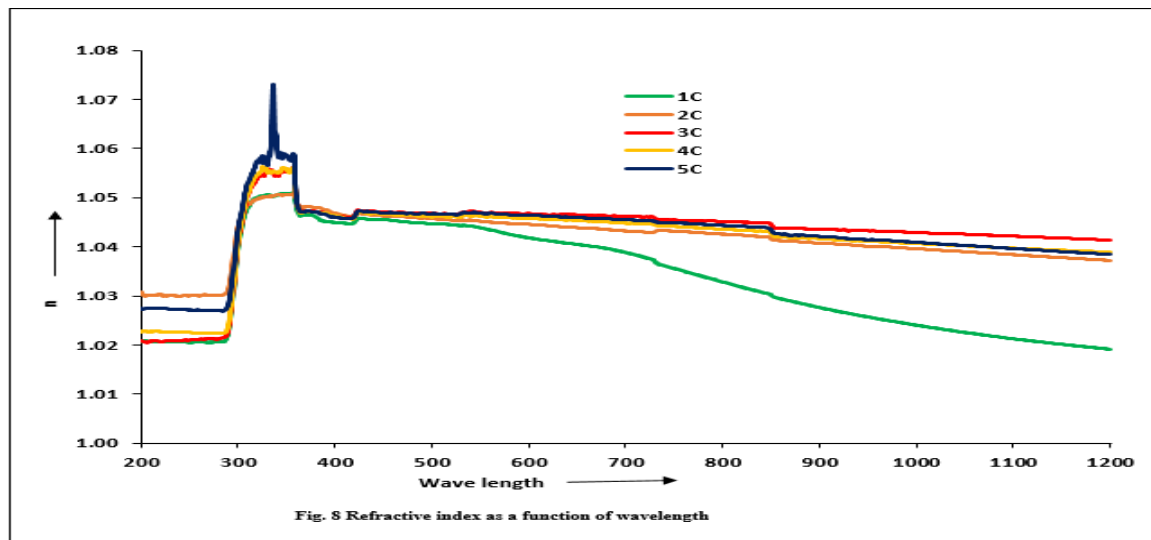
Fig.7.TGA Curve

E. Refractive Index

The refractive index has been calculated using the relation reported by Islam and podder [13].

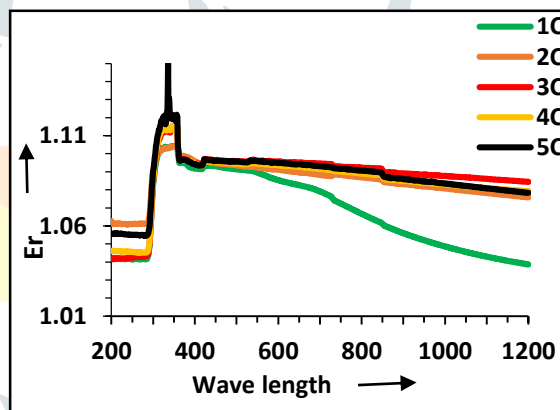
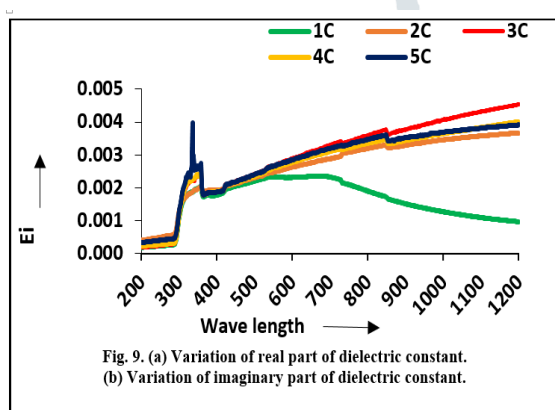
$$n = \left(\frac{1 + R}{1 - R} \right)$$

Where n is the refractive index and R is the optical reflectance. The variation of refractive index with wave length for different number of coat as shown in fig. 8. From fig. 7 it is evident that refractive index between 1.02 to 1.07 in the visible region, means that electromagnetic radiation is 2-2.58 time slower in the oxide films than in the free space [13] and increases with the increase in thickness of the film, which is in good agreement. Here thin films by varying number of coat we obtain value of refractive index is 1.02 to 1.07. Refractive index rapidly increases between the wavelength 280 nm to 350 nm and then it gradually decreases. Low refractive index occurs due to successive internal reflection or due to the trapped photon energy with the grain boundary. It is also attributed to the variety of impurities and defects with the increase of the thickness of the film and this implies that there is a strong optical scattering.



F. Dielectric constant

The real ϵ_r and imaginary ϵ_i parts of dielectric constant were determined using the formula $\epsilon_r = n^2 - k^2$ and $\epsilon_i = 2nk$. The variation of the real and imaginary parts of the dielectric constant for different number of coat is illustrated in Fig. 9(a) and 9(b). Fig. 9(a) and 9(b) revealed that the value of the real part 1.03 – 1.16 is higher than that of the imaginary part.

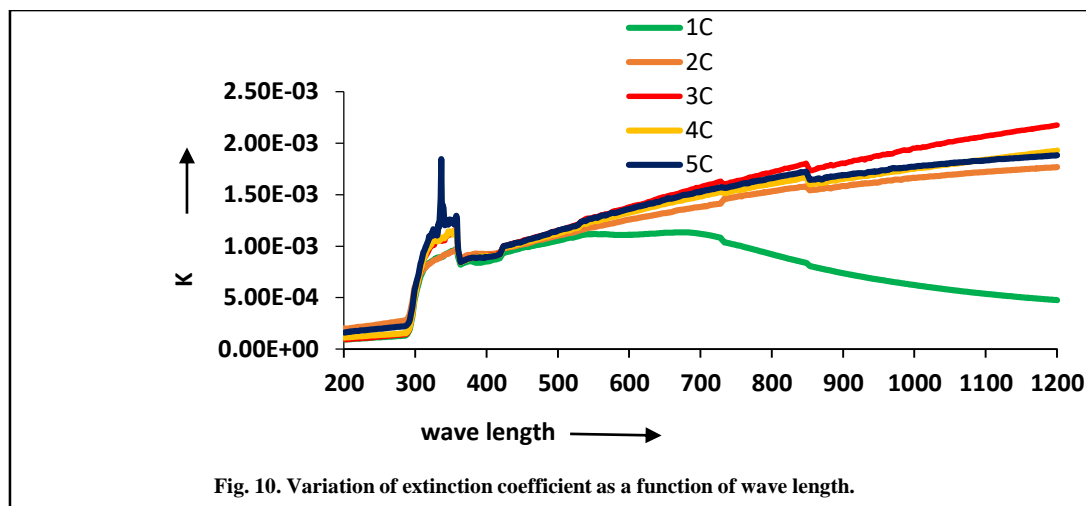


G. Extinction coefficient

The extinction coefficient of the zinc oxide thin films were determined from absorbance measurements. The extinction coefficient k can be obtained from the experimental expressions:

$$k = \left(\frac{\alpha \lambda}{4\pi} \right)$$

The refractive index (n) provide the optical properties of the film. The variation of extinction coefficient with wave length is shown in Fig. 10. The rise and fall in the extinction coefficient is directly related to the absorption of light [13]. From Fig. 10 it is clear that K increases rapidly with increasing wavelength from 300 to 350 nm and after that value of K gradually increases.



IV CONCLUSIONS

ZnO thin films have been successfully deposited with different morphologies with (100), (002), (101), (102), (110), (103) and (200) preferential orientation using a chemical bath deposition technique onto a glass substrate. The synthesis of zinc oxide nanoparticles from a zinc chloride by a thermal decomposition technique was studied in this paper. ZnO hexagonal wurtzite structure were successfully synthesized by a low cost not require high technology equipment's simple one step and without catalyst or buffer layer on substrate with high quality product. The band gap of the film is 4.26 eV to 4.30 eV. Refractive index is 1.02 – 1.07. Value of the real part of dielectric constant is 1.03- 1.16. Hexagonal wurtzite morphology showed in SEM images.

REFERENCES

- [1] G. Neri, A. Bonavita, G. Rizzo, S. Galvano, N. Pinna, M. Niederberger, S. Capone, P. Siciliano, 2007. "Chemical route to synthesis of mesoporous ZnO thin films and their liquefied petroleum gas sensor performance". *Sens. Actuators B*, pp.564.
- [2] D.S. Dhawale, R.R. Salunkhe, V.J. Fulari, M.C. Rath, N.S. Sawant, C.D. Lokhande, 2009. "Enhanced gas sensing properties by SnO₂ Nano sphere functionalized TiO₂ Nano belts". *Actuators B*, pp.58.
- [3] V.R. Shinde, T.P. Gujar, C.D. Lokhande, 2007. "Nanostructured Zinc Oxide". *Sens. Actuators B*, pp.551.
- [4] R.R. Salunkhe, D.S. Dhawale, D.P. Dubal, C.D. Lokhande, 2009. "Sprayed CdO thin films for liquefied petroleum gas (LPG) detection", *Sens. Actuators B*, pp.86.
- [5] Zhang, Y.; Mu, J. "Controllable synthesis of flower- and rod-like ZnO nanostructures by simply tuning the ratio of sodium hydroxide to zinc acetate", *Nanotechnology*, 18, pp.075606.
- [6] U. Ozgur, Y.I. Alivov, C. Liu, A. Teke, M.A. Reshchikov, S. Dogan, V. Avrutin, S.J. Cho, H. Morkoc. 2005 "A comprehensive review of ZnO materials and devices", *J. Appl. Phys.*, pp.041301.
- [7] D.S. Dhawale, D.P. Dubal, A.M. More, T.P. Gujar, C.D. Lokhande, 2010. "Room temperature liquefied petroleum gas (LPG) sensor", *Sens. Actuators B*, pp.488.
- [8] J. Chen, Jin Li, G. Jiahui Li, X. Xiao, J. Yang, *J. Alloys Compd.*, 2011, pp.740.
- [9] A. Forleo, L. Francioso, S. Capone, P. Siciliano, P. Lommens, Z. Hens, 2010. "Room-temperature solid state synthesis of ZnO/ α -Fe₂O₃ hierarchical nanostructures and their enhanced gas-sensing properties", *Sens. Actuators B*, pp.111.
- [10] Kang-Min Kim, Hae-Ryong Kim, Kwon-II Choi, Hyo-Joong Kim, Jong-Heun Lee, 2011. "Design of Highly Sensitive C₂H₅OH Sensors Using Self-Assembled ZnO Nanostructures", *Sensors*, pp.9685-9699.
- [11] Kang-Min Kim, Hae-Ryong Kim, Kwon-II Choi, Hyo-Joong Kim, Jong-Heun Lee, 2011. "ZnO hierarchical nanostructures grown at room temperature and their C₂H₅OH Sensor applications", *Sensors and Actuators B*, pp.745–751.
- [12] Y.X. Du, Q.X. Yuan, *J. Standing*, 2010. "Porous ZnO Nano plate-built hollow microspheres", *Alloys Compd.*, pp.468.
- [13] D. Bao, H. Gu, A. Kuang, 1988. "Sol gel-derived C-axis oriented ZnO thin films", *Thin Solid Films*, pp.37-39.
- [14] Babita, B, Kishore Kumar, D. Manorama, 2006. "SV: Hydrothermal synthesis of highly crystalline ZnO nanoparticles: a competitive sensor for LPG and EtOH" *Sens. Actuators B.*, pp.676–682.